



This is an author produced version of a paper published in Dalton Transactions: the international journal for inorganic, organometallic and bioinorganic chemistry.

This paper has been peer-reviewed but may not include the final publisher proof-corrections or pagination.

Citation for the published paper:

Lars Eklund, Tomas S. Hofer, Alexander K. H. Weiss, Andreas O. Tirlir and Ingmar Persson. (2014) Structure and water exchange of the hydrated thiosulfate ion in aqueous solution using QMCF MD simulation and large angle X-ray scattering. *Dalton Transactions: the international journal for inorganic, organometallic and bioinorganic chemistry*. Volume: 43, Number: 33, pp 12711-12720.  
<http://dx.doi.org/10.1039/C4DT01010H>.

Access to the published version may require journal subscription.  
Published with permission from: Royal Society of Chemistry.

Epsilon Open Archive <http://epsilon.slu.se>

# Structure and water exchange of the hydrated thiosulfate ion in aqueous solution using QMCF MD simulation and large angle X-ray scattering

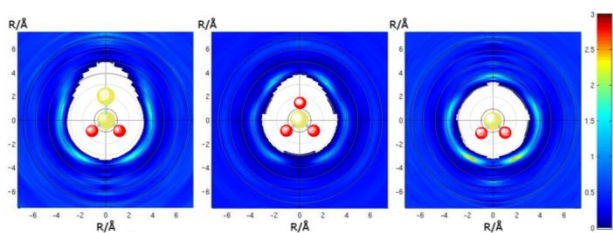
Lars Eklund,<sup>a</sup> Tomas S. Hofer,<sup>b</sup> Alexander K. H Weiss,<sup>b</sup> Andreas O. Tirlir,<sup>b</sup> and Ingmar Persson<sup>a,\*</sup>

<sup>a</sup> Department of Chemistry and Biotechnology, Swedish University of Agricultural Sciences, P.O.Box 7015, SE-750 07 Uppsala, Sweden.

<sup>b</sup> Theoretical Chemistry Division, Institute of General, Inorganic and Theoretical Chemistry, University of Innsbruck, Innrain 80-82, A-6020 Innsbruck, Austria.

† Electronic supplementary information (ESI) available. Summary of S-O and S-S bond distances in solid state structures containing  $\text{S O}_x^{2-}$ ,  $x=3-8$ , and radial distribution functions from simulation of the thiosulfate ion, and from experimental LAXS data on the hydrated peroxodisulfate ion in water.

## Graphical Abstract



## Synopsis

Experimental and simulation data of the thiosulfate ion show large similarities in hydration structure and mechanism with the sulfate ion but with weaker hydration of the terminal sulfur atom in thiosulfate.

## Abstract

Theoretical *ab initio* quantum mechanical charge field molecular dynamics (QMCF MD) has been applied in conjunction with experimental large angle X-ray scattering (LAXS) to study the structure and dynamics of the hydrated thiosulfate ion,  $S_2O_3^{2-}$ , in aqueous solution. The S-O and  $S_C-S_T$  bond distances have been determined to 1.479(5) and 2.020(6) Å by LAXS and to 1.478 and 2.017 Å by QMCF MD simulations, which are slightly longer than the mean values found in the solid state, 1.467 and 2.002 Å, respectively. This is due to the hydrogen bonds formed at hydration. The water dynamics show that water molecules are exchanged at the hydrated oxygen and sulfur atoms, and that the water exchange is ca. 50% faster at the sulfur atom than at the oxygens atoms with mean residence times,  $\tau_{0.5}$ , of 2.4 and 3.6 ps, respectively. From this point of view the water exchange dynamics mechanism resembles the sulfate ion, while it is significantly different from the sulfite ion. This shows that the lone electron-pair in the sulfite ion has a much larger impact on the water exchange dynamics than a substitution of an oxygen atom for a sulfur one. The LAXS data did give mean  $S_C \cdots O_{aq1}$  and  $S_C \cdots O_{aq2}$  distances of 3.66(2) and 4.36(10) Å, respectively, and  $S_C-O_{thio}$  and  $O_{thio} \cdots O_{aq1}$ ,  $S_C-S_T$  and  $S_T \cdots O_{aq2}$  distances of 1.479(5), 2.845(10), 2.020(6) and 3.24(5) Å, respectively, giving  $S_C-O_{thio} \cdots O_{aq1}$  and  $S_C-S_T \cdots O_{aq2}$  angles close 110°, strongly indicating a tetrahedral geometry around the terminal thiosulfate sulfur and the oxygens, and thereby, three water molecules are hydrogen bound to each of them. The hydrogen bonds between thiosulfate oxygens and the hydrating water molecules are stronger and with longer mean residence times than between water molecules in the aqueous bulk, while the opposite is true for the hydrogen bonds between the terminal thiosulfate sulfur and the hydrating water molecules. The hydration of all oxo sulfur ions are discussed using the detailed observations for the sulfate, thiosulfate and sulfite ions, and the structure of the hydrated peroxodisulfate ion,  $S_2O_8^{2-}$ , in aqueous solution has been determined by means of LAXS to support the general observations. The mean S-O bond distances are 1.448(2) and 1.675(5) Å to the oxo and peroxy oxygens, respectively.

## Introduction

The hydration of chemical species is essential for all chemical reactions taking place in e.g. aqueous media and moist air. The hydration of anions is normally weaker than for most cations due to their lower charge density,<sup>1</sup> and the water exchange rate is normally faster for the same reason. The effects of hydration is however not limited to the local effect of interactions with the hydrated ion itself but also with the macroscopic properties of the solution. This paper is the third in a series where the hydration of oxosulfur anions in aqueous solution is investigated from structural and water exchange point of view.<sup>2,3</sup> The water exchange rate of these anions is so fast that they can be not determined experimentally, and instead the best way to get such information is through high level simulations, which also give insights of the water exchange mechanism. Structures of chemical species in solution, including distances and geometries, can be determined by EXAFS, large angle X-ray scattering (LAXS) or large angle neutron scattering. The previous studies on the sulfate and sulfite ions have shown that the water exchange mechanisms are very different for the highly symmetric sulfate ion ( $T_d$ ) and the sulfite ion with lower symmetry ( $C_{3v}$ ) due to the presence of a lone electron-pair.<sup>2,3</sup> The water exchange in the hydrated sulfate ion takes place in a direct exchange reaction at the sulfate oxygens,<sup>3</sup> and the mean residence time, MRT, is 2.6 ps which is slightly longer than between water molecules in the aqueous bulk, 1.7 ps.<sup>4</sup> On the other hand, the water exchange mechanism of the hydrated sulfite ion is more complex and takes only place in close vicinity of the lone electron-pair directed at its sides, and in principle no water exchange takes place at the sulfite oxygens.<sup>2</sup> The MRT of the hydrated sulfite is slightly longer, 3.2 ps, than for the sulfate ion. However, the MRT of the sulfite ion shall not be compared with e.g. the sulfate ion due to the complex water exchange mechanism of the latter.<sup>2</sup> Three water molecules are hydrogen bonded to each sulfate and sulfite oxygen in the hydrated sulfate and sulfite ions in aqueous solution.<sup>2,3</sup> The S-O bond distances in the hydrated sulfate and sulfite ions are slightly longer than in solid anhydrous salts due to the hydration.<sup>2,3</sup>

In this paper the structure and the water exchange dynamics of the thiosulfate ion in aqueous

solution will be presented. The terminal sulfur atom in the thiosulfate ion is expected to be more weakly hydrated than oxygen atoms. Whether such an asymmetric hydration will affect the water exchange mechanism, as it does for the sulfite ion, is a point of particular interest in this study. The thiosulfate ion is proposed to be asymmetrically hydrated in a recent simulation study,<sup>5</sup> with the water molecules more strongly hydrogen bound to the oxygens ( $O_{\text{thio}}$ ) than to the terminal sulfur ( $S_{\text{T}}$ ). It was reported that the terminal sulfur atom has hydrophobic properties, and that the  $S_{\text{C}}-S_{\text{T}}$  bond is shorter in aqueous solution than in the solid state.<sup>5</sup> The weaker hydration of the  $S_{\text{T}}$  atom is suggested to be the reason in its role as the active site in chemical reactions.<sup>5</sup> These statements are surprising and need to be verified by independent high level simulations and experimental structure determination in aqueous solution. Thiosulfate is regarded as a typical soft electron-pair donor forming strong complexes to typically soft electron-pair acceptors through its terminal sulfur atom.<sup>6</sup> This property is used in many chemical and technical applications as removal of silver compounds,<sup>7</sup> and as a possible replacement for cyanide in gold extraction.<sup>8</sup> The role of thiosulfate in biochemistry is well established.<sup>9</sup>

The aim of this study is to determine the structure of the hydrated thiosulfate ion in aqueous solution with LAXS and to make an extensive analysis of a quantum mechanical charge field molecular dynamics (QMCF MD) simulation with emphasis on structure and water exchange dynamics. This includes a check of the statements of the terminal thiosulfate sulfur having hydrophobic properties and that the S-S bond distance is shorter in aqueous solution than in solid state. A comparison of the hydration of the sulfate, sulfite and thiosulfate ions in aqueous solution from structural and water exchange mechanism and dynamics point of view will be made in order to find out if there is any relationship between hydration properties, symmetry, oxidation state of the central sulfur atom and electron distribution of the ion. The sulfate, sulfite and thiosulfate ions represent a series of oxo anions with a full shell of oxygens (sulfate), a lone electron-pair instead of one oxygen in one apex in a tetrahedral configuration (sulfite) and with substitution of one of the oxygens for a sulfur (thiosulfate). The structure of the hydrated peroxodisulfate ion has been

determined in aqueous solution for a further comparison of hydration of sulfur oxo acids where the oxo group has been exchanged for a peroxy group.

## Experimental

**Chemicals.** Sodium thiosulfate pentahydrate,  $\text{Na}_2\text{S}_2\text{O}_3 \cdot 5\text{H}_2\text{O}$  (Sigma-Aldrich, analytical grade), sodium peroxodisulfate,  $\text{Na}_2\text{S}_2\text{O}_8$  (Merck, analytical grade), and sodium hydroxide,  $\text{NaOH}$  (Sigma-Aldrich, analytical grade), were used without further purification.

**Solution.** The solutions for the LAXS experiment were prepared by dissolving a weighed amount of sodium thiosulfate or peroxodisulfate in Milli Q filtered water, and pH was adjusted to 12.0 by addition of a small amount of sodium hydroxide to final concentrations of 1.5066 and 1.5000  $\text{mol} \cdot \text{dm}^{-3}$ , respectively, giving densities of 1197.3 and 1304.8 g/L and the water concentrations were 53.237 and 52.602  $\text{mol} \cdot \text{dm}^{-3}$ , respectively.

**Large Angle X-ray Scattering (LAXS).** The scatter of  $\text{MoK}\alpha$  X-ray radiation,  $\lambda=0.7107 \text{ \AA}$ , from the free surfaces of the aqueous disodium thiosulfate and peroxodisulfate solutions were measured in a large angle  $\theta$ - $\theta$  goniometer described elsewhere.<sup>10</sup> A flat measuring surface of the irradiated area was obtained by filling a Teflon cup until a positive meniscus was observed and sealing it in an airtight measuring chamber with beryllium windows. A  $\text{LiF}(200)$  single crystal focusing monochromator was used to monochromatize the scattered radiation. The scattering was determined at 450 discrete angles in the angle range of  $0.5 < \theta < 65^\circ$ , where the scatter angle is  $2\theta$ . 100,000 X-ray quanta were collected for each angle, and the entire angle range was scanned twice corresponding to a statistical error of about 0.3 %. A combination of divergence-collecting-focal slits of  $1/4^\circ$ - $1/2^\circ$ -0.2 mm and  $1^\circ$ - $2^\circ$ -0.2 mm defining the X-ray beam were applied with the smaller slits for  $\theta < 10^\circ$  and the larger for  $\theta > 10^\circ$ . To get a suitable counting rate and change in angle, data was collected in three different  $\theta$ -regions, with overlapping regions to enable scaling of the data. The details of data collection and treatment are described elsewhere.<sup>10</sup> The KURVLR software<sup>11</sup> was used for the data treatment, The structural parameters contained in the theoretical model where

refined by minimizing  $U = w(s)\sum s^2 [i_{\text{exp}}(s) - i_{\text{calc}}(s)]^2$  using the STEPLR program.<sup>12,13</sup> Normalization of the data to one stoichiometric unit containing two sulfur atoms using the scattering factors  $f$  for neutral atoms, including corrections for anomalous dispersion,  $\Delta f'$  and  $\Delta f''$ ,<sup>14</sup> Compton scattering<sup>15,16</sup> and multiple scattering events. The multiple scattering events play a significant role in the scatter from solutions with low molar absorption coefficient, for the studied solutions  $\mu = 2.396$  and  $2.534 \text{ cm}^{-1}$ , respectively. To make peak widths comparable with data from the QM/MD simulations the temperature factors were recalculated as full width half height, fwhh, assuming Gaussian distributed peaks, then  $b=l^2/2$  gives  $\text{fwhh}=\sqrt{(\ln 2 * 2)} * \sqrt{2 * b}$ .

**Quantum Mechanical Charge Field Molecular Dynamics (QMCF MD).** As common in hybrid quantum mechanical/molecular mechanical (QM/MM) approaches,<sup>17-23</sup> the simulation systems is separated into a high- and a low-level zone. While the interactions within the first region are treated by application of a suitable quantum chemical technique, classical potential functions are considered to be sufficiently accurate to describe the remaining part of the system. In addition the QMCF approach<sup>24,25</sup> exploits the fact that non-Coulombic interactions become negligible at relatively small distances. Thus, for atoms located in the center of the quantum mechanical region, the application of these non-Coulombic contributions in the QM/MM coupling can be safely neglected, provided that the size of the QM region is sufficiently large. To achieve this, the QM region is further separated into a core and layer zone when evaluating the QM/MM coupling potentials. In addition the application of the electrostatic embedding technique to account for the influence of the partial charges of the MM atoms surrounding the quantum mechanical zone was found to significantly improve the description of the system. To enable the migration of molecules between the high- and low-level zone, a smoothing procedure is applied to continuously shift the forces from the QM to MM contribution and *vice versa*. Further details regarding the QMCF technique can be found elsewhere.<sup>24-26</sup>

*Simulation protocol.* The molecular simulations was carried out using periodic boundary condition in a cubic box with the edge length of 24.1 Å containing 500 water molecules, which corresponds to a density of 0.997 g·cm<sup>-3</sup>. The target temperature of 298 K was kept constant via the Berendsen weak coupling algorithm.<sup>27,28</sup> To account for the error associated to the application of a Coulombic cut-off set to 12.0 Å the reaction field approach was employed.<sup>29</sup> The equations of motion were treated via the velocity Verlet algorithm<sup>29</sup> employing a time-step of 0.2fs, data sampling has been performed every fifth time-step. Based on their centers of mass, molecules within a radius of 7.3 Å from the central sulfur atom (S<sub>C</sub>) are included into the QM region. This distance was chosen considering the average distances obtained from the LAXS measurements to ensure that the complete asymmetric shell is treated quantum mechanically. Since the application of the QMCF approach resulted in very good agreement with experimental data in previous investigations of simulated systems<sup>2,3</sup>, at the Hartree-Fock/Dunning double zeta plus polarization (DZP) level,<sup>30,31</sup> the same level of theory and basis set was chosen for this simulation. The simple model produces a good result and sufficient number of simulation steps within a reasonable production time of approximately one year, using 4 AMD 2382 quad-core processors (16 cores) executing the quantum chemical computations in parallel with the TURBOMOLE 6.4 software package.<sup>32</sup> In order to assess the quality of the chosen level of theory in the case of the thiosulfate ion, a comparison of the minimum structures obtained for [S<sub>2</sub>O<sub>3</sub>.H<sub>2</sub>O]<sup>2-</sup> via energy minimization in implicit solvent at HF, MP2 and CCSD level have been carried out (see Table S1 and Figure S1, ESI†), confirming that the HF level provides an adequate compromise between accuracy of results and computational effort. To describe the solvent-solvent interaction between MM molecules as well as in the QM/MM coupling the flexible BJH-CF2 water model was used,<sup>33,34</sup> since it explicitly takes intramolecular hydrogen modes into account. The simulation ran 8 ps for equilibration and 20 ps for sampling.

### **Analysis methods of the QMCF simulation**

The simulation trajectory has been analyzed in terms of radial distribution functions (RDFs),

angular-radial-distributions (ARDs), spatial density projections, as well as mean lifetime analyses of ligand exchanges and hydrogen bonds. Typically, the RDF obtained from simulations is expressed as  $g(r) = V/N^2 \langle n(r, \Delta r) \rangle_M / 4\pi r^2 \Delta r$ , while the experimental RDF is given as  $D(r) - 4\pi r^2 \rho_o$ .

Using angularly overlapping conical regions with a central vector along the  $C_{3v}$  axis a function of distance and angle,  $D(r, \alpha)$ , an angular radial distribution function (ARD) is defined where  $\alpha$  is the angle of the conical region with respect to the central axis, in this case the step in  $\alpha$  was  $22.5^\circ$ . The ARD can then be used to compare water distributions of the hydration sphere with other ions.

The particle density of the water oxygen population in the surrounding of the solute was computed and projected onto a set of planes perpendicular to the  $C_{3v}(S_2O_3)$  axis, having a  $1.0 \text{ \AA}$  spacing starting with a plane centered at the central sulfur atom ( $S_c$ ). The resulting projections yield detailed information about the spatial density in the vicinity of the solute [spatial density].<sup>35</sup>

Mean ligand residence times (MRT)  $\tau$  were analyzed using a direct measurement of exchange events.<sup>36</sup> By registering all border crossing events  $N_{ex}^{0.5}$  lasting for a duration of  $t^* = 0.5\text{ps}$ ,<sup>36</sup> the mean residence time is obtained as  $\tau^{0.5} = CN_{av} N_{ex}^{0.5} / t_{sim}$  where  $CN_{av}$  and  $t_{sim}$  correspond to the average coordination number and the total simulation time respective. The ratio of exchanges  $R_{ex}$  obtained as the quotient of the number of registered exchange events and the number of all occurring border crossings  $N_{ex}^{0.0}$  (registered for  $t^* = 0.0\text{ps}$ ) corresponds the average number of border crossing attempts to achieve one lasting exchange event.

The hydrogen bond lifetimes can be analyzed with two correlation functions, the intermittent

hydrogen bond correlation function  $C_{HB}(t) = \frac{\langle h(0)h(t) \rangle}{\langle h \rangle}$  and the continues hydrogen bond correlation

function  $S_{HB}(t) = \frac{\langle H(0)H(t) \rangle}{\langle H \rangle}$  where  $h(0)$  is the hydrogen bond population at time zero and  $h(t)$  the

corresponding population at time t and  $H(0)$  and  $H(t)$  are analogous but not allowing for reforming of the hydrogen bond. The hydrogen population is defined depending on distance and angle between the  $X \cdots H-O$ . To allow for thermal movements the hydrogen bond angle was allowed to deviate from

180° with 35° and distance was determined based on the acceptor atom either oxygen or sulfur. The  $C_{HB}(t)$  term was fitted as a two part exponential decay with a short and a long component  $\tau_1$  and  $\tau_2$ ,  $C_{HB}(t) = a_0 e^{-t/\tau_1} + (1 - a_0) e^{-t/\tau_2}$  the same type of double exponential was fitted for the S(t) where the long parameter is a measure of the hydrogen bond life time. Visual modelling was conducted using VMD.<sup>37</sup>

## Results and Discussion

### *Structure of the hydrated thiosulfate ion in aqueous solution*

The experimental radial distribution function (RDF) from the LAXS measurement of the aqueous sodium thiosulfate solution shows peaks at 1.5, 2.0, 2.85 and 3.8 Å, Figure 1. The weak peaks at 1.5 and 2.0 Å correspond to the S-O and S-S bond distances within the thiosulfate ion, and the peak at 3.8 Å corresponds to  $S_C \cdots O_{aq1}$  and  $S_C \cdots O_{aq2}$  distances. The strong peak at 2.85 Å contains several interactions including  $O_{thio} \cdots O_{aq1}$  and  $S_T \cdots O_{aq2}$  in the hydrated thiosulfate ion, and the mean  $O_{aq} \cdots O_{aq}$  distance in the aqueous bulk. The refined  $S_C \cdots O_{aq1}$  and  $S_C \cdots O_{aq2}$  distances of 3.66(1) and 4.36(6) Å, respectively, and the  $S_C-O_{thio}$  and  $O_{thio} \cdots O_{aq1}$ , and  $S_C-S_T$  and  $S_T \cdots O_{aq2}$  distances of 1.479(5), 2.845(10), 2.020(6) and 3.24(5) Å, respectively, give  $S_C-O_{thio} \cdots O_{aq1}$  and  $S_C-S_T \cdots O_{aq2}$  angles close to 110°, thus, a tetrahedral geometry around the terminal thiosulfate sulfur and oxygens. Therefore, most likely three water molecules are hydrogen bound to each sulfur and oxygen, in total twelve water molecules are hydrating the thiosulfate ion in aqueous solution. The structure of the hydrated sodium ion was modeled as a regular octahedron with Na-O bond distances of 2.42(2) Å, which is in full agreement with previously reported distance.<sup>38</sup> The refined structure parameters from the LAXS measurement are summarized in Table 1, and the experimental and the calculated RDFs using the parameters given in Table 1 are shown in Figure 1 together with the individual contributions from the hydrated thiosulfate and sodium ions and the aqueous bulk.

The QMCF MD simulation resulted in structure parameters in excellent agreement with the experimental ones, Table 1 and Figure S2 (see ESI†). The  $S_C-O$  and  $S_C-S_T$  bond distances within the hydrated thiosulfate ion are in exceptional good agreement between experiment and simulation,

the bond distance distributions are significantly narrower in the simulation than from the LAXS experiment, Table 1. The bond distances within the thiosulfate ion are furthermore in very good agreement with distances reported solid state structures reported in the literature on average 1.467 and 2.002 Å; selected structures containing uncoordinated thiosulfate ions are summarized in Table S2 (see ESI†). The mean S-O and S-S bond distances are slightly longer in the hydrated thiosulfate ion in aqueous solution due to the hydrogen bonding to the terminal sulfur and oxygens.

#### *Water exchange dynamics of the thiosulfate ion in aqueous solution*

The angular radial distribution (ARD) plot for a plane cutting through the ion along an axis of symmetry shows the distribution of distances as a function of angle. The  $g(r, \alpha)_{S-O}$  is proportional to the population of water oxygen, Figure 2. For sulfate (center) a narrow symmetric distribution in both distance and angle for a large value of  $g(r)_{S-O}$  shows a symmetric exchange and a direct interaction of the water molecules. A similar feature is seen for the thiosulfate oxygens (Figure 2, left) also with a clear direct exchange between bulk water and hydration shell. The water molecules hydrogen bound the terminal sulfur,  $S_T$ , exhibit a broader in distribution with more rapid exchange events. There is a significant difference in the distribution function of the hydration shell of the sulfite ion as the lone pair, weakly interacting with water molecules, give rise to a different exchange mechanism there no directed water exchange between the bulk and the hydration shell seen by no well-defined distances in this region (Figure 2, right). Distinguishing the migration pathways was done by angle-distance plot (Figure 3, left) which show regions with higher and lower densities of migration paths coinciding with loci for hydrogen bonding as seen in the ARD. For the thiosulfate no molecular mean residence time (MRT) was analyzed, this was because the MRT analysis is spherical and to give a meaningful definition of border crossings in the simulation and no sphere centered on  $S_C$  would give an interpretable result. This is because it cannot cross the minima outside the first shell on both oxygen side and terminal sulfur side as shown by the ARD (Figure 2). To compare with earlier studies<sup>5</sup> the atomic MRT was evaluated by selecting a region centered on each atom of the ion, the asymmetric contributions are observed. The asymmetry of the

hydration shell of thiosulfate is further demonstrated by the MRT on each of the thiosulfate oxygens and the terminal sulfur, Table 2; MRTs for the sulfate, sulfite and phosphate ions in water and in bulk is summarized in Table 3. The water molecules clustered around the terminal sulfur has a higher exchange rate requiring ca. 45 attempts per successful exchange lasting longer than 0.5 ps, while the waters around the oxygens only 14-20 attempts are needed. The sustainability of the waters hydrogen bound to thiosulfate oxygens of thiosulfate are comparable to those of bulk water, while the MRT was about double and the number of exchanges lower for a successful exchange event lasting longer than 0.5 ps. The MRT for the water molecules hydrogen bound to the sulfur atom,  $S_T$ , is only about 1.5 of that for bulk water and the number of exchanges needed was much higher, about twice that of bulk water. This leads to a sustainability at the  $S_T$ , which is about half of a bulk water interaction. The hydrogen bond strength as determined via  $C_{HB}(t)$  and  $S_{HB}(t)$  to the sulfur atom is sufficiently weak to regard that the  $S_T$  site acts as a weak structure breaker, while the hydrogen bonds to the oxygens are sufficiently strong to regard those sites as structure makers, giving the thiosulfate ion overall weak structure maker properties, though asymmetric. The hydrogen bond lifetime are determined by evaluating the hydrogen bond auto correlation functions  $C_{HB}(t)$ ,  $S_{HB}(t)$  (Figure 3, right), results in table 4, for the oxygens also confirms that they are weak structure makers. The hydrogen bond lifetime of  $S_T$  was about half that of the oxygen at 1.16 ps and therefore it can be confirmed as a weak structure breaker. The results obtained in this study both MRT and Hydrogen bond correlation functions were in contrast to the conclusions presented by Trinapakul et al.<sup>5</sup>, who reported unexpected results with the terminal thiosulfate sulfur having hydrophobic properties and with a S-S bond distance shorter in aqueous solution than in solid state. This study clearly shows that significant hydrogen bonds are formed between water and the terminal thiosulfate sulfur even though they are weaker than the hydrogen bonds in bulk water. Furthermore, the slightly longer S-S bond in aqueous solution than in solid state shows that the hydrogen bonding slightly weakens and lengthens the S-S bond, as expected, Table 1. A possible explanation for the unexpected results reported by Trinapakul et al. may be that they used a QM

region diameter of 6.0 Å, whereas in this study the QM region of 7.3 Å, was chosen, ensuring that the entire water peak clustered outside the  $S_T$  is included in the QM core.

By averaging the atomic particle distributions on top of a volume map, the density of the core ion and the first hydration shell is clearly seen, Figure 4. The population analysis of the oxygen densities with the solute over-layed in RGB color scheme over the solvent in CMYK color scheme and the central image is a plane that cuts through the center of  $S_C$ , Figure 5. It shows an increased mobility (wider spread densities) in the hydration shell as one goes up and out (left and up) along the  $C_{3v}$  axis towards the terminal sulfur ( $S_T$ ), and with more rigid hemispherical densities as one goes down, right and down in the figure. The analysis show a clear indication of higher ordered structure of the water molecules around the thiosulfate oxygens than around the  $S_T$  sulfur showing a slight asymmetry the hydration shell order as also indicated by the ARD.

In order to obtain an estimate for the overall coordination number, each oxygen atom located within the vicinity of either an oxygen or the terminal sulfur atoms of thiosulfate has been registered in every frame of the simulation. The resulting average coordination number of 12.5 agrees very well with the experimental value, with coordination numbers 12 and 13 marking the most frequent numbers of first shell ligands observed along the simulation (see Figure 6). The deviation of the average value of 12.5 from the integer coordination number of 12 can be explained by the large number of ligand exchange events, being a result of the dynamic description of the system.

### ***General aspects of hydrated oxosulfur anions in aqueous solution***

The structures and water exchange dynamics of the sulfite,<sup>3</sup> sulfate<sup>2</sup> and thiosulfate ions in aqueous solution have been studied by QMCF MD simulations and LAXS experiments. Even though only three ions have been studied clear principles of the hydration structures and dynamics emerge. For these three ions three water molecules are hydrogen bound to the oxygen atoms in tetrahedral configuration, and these hydrogen bonds are stronger and with longer mean residence time than the

hydrogen bonds in pure water, thus, they are regarded as structure makers. From LAXS and DDIR studies on the selenite, selenate,<sup>41</sup> arsenite and arsenate ions and telluric acid<sup>38</sup> it is observed that the hydration from structural point of view is the same even though one or several of the oxygens are protonated, even though these protons act as hydrogen bond donors. It can therefore be assumed that from structural point of view also the oxo sulfur anions maintain their hydration structure at protonation. Regarding the water exchange dynamics, the oxo sulfur anions with a tetrahedrally coordinated central sulfur atom, sulfate and thiosulfate ions, a direct water exchange mechanism between hydrated water molecules and water molecules in the aqueous bulk is observed.<sup>2</sup> On the other hand, at the presence of a lone electron-pair, as in the sulfite ion, a more complex water exchange mechanism is observed with in principle no exchange at oxygen atoms, and instead water molecules are transported to area close to the lone electron-pair where it is exchanged and the exchanged is then transported to the oxygen.<sup>2</sup> The central sulfur atom in the oxo sulfur anions dithionate or metabisulfate,  $S_2O_6^{2-}$ , disulfate or pyrosulfate,  $S_2O_7^{2-}$ , and peroxodisulfate,  $S_2O_8^{2-}$ , is tetrahedrally coordinated. It is therefore expected that these ion have a hydration structure around the oxygen atoms and a water exchange mechanism similar to the sulfate ion as only oxygen atoms can hydrogen bind hydrating water molecules. This has in part been confirmed by LAXS study of the peroxodisulfate ion, see below. On the other hand, the dithionite,  $S_2O_4^{2-}$ , and disulfite or metabisulfite,  $S_2O_5^{2-}$ , ions have lone electron-pair on both and one of the sulfur atoms, respectively, and the water exchange mechanism is expected to more complex and similar to the sulfite ion. The reported structures of the dithionite, disulfite, dithionate, disulfate and peroxodisulfate ions in solid state are summarized in Table S3 (see ESI†). It can be assumed that these ions maintain their structure in solid state also in aqueous solution, but with a slight increase, 0.1-0.02 Å, in the S-O bond distances, and in the  $S_C-S_T$  bond distances in the dithionite and disulfite ions, due to the hydration. The oxo sulfur anions can most likely be regarded as structure makers with stronger hydrogen bonds with longer mean residence time between the oxygen atoms and hydrating water molecules than in pure water. However, the thiosulfate ion shows that the hydrogen bonds between

the terminal sulfur and the hydrating water molecules is weaker than in pure, and that within the same ion both structure making and breaking properties can be present, but the overall behavior is structure making. It can be assumed that the dithionite and disulfite ions behave from this point of view as the thiosulfate ion.

#### *Structure of the hydrated peroxodisulfate ion in aqueous solution*

The experimental RDF of LAXS data of an aqueous solution of sodium peroxodisulfate shows peaks at 1.45, 2.9 and 3.8 Å, Figure S3 (see ESI†). The weak peak at 1.5 Å correspond to the S-O bond distance to the oxo oxygens within the peroxodisulfate ion and the S-O bond distance to the peroxy oxygens is seen as a weak shoulder at ca. 1.7 Å. The peak at 3.8 Å corresponds to the  $S_{\text{oxo}} \cdots O_{\text{aq}}$  distance. The strong peak at 2.9 Å contains several interactions including  $O_{\text{oxo}} \cdots O_{\text{aq}}$  and the mean  $O_{\text{aq}} \cdots O_{\text{aq}}$  distance in the aqueous bulk. The S- $O_{\text{oxo}}$  and S- $O_{\text{peroxy}}$  distances were refined to 1.448(2) and 1.674(6) Å, respectively, which is slightly longer than observed in the solid state, 1.424 and 1.641 Å, respectively. Table S3 (see ESI†). The  $O_{\text{oxo}} \cdots O_{\text{aq}}$  and  $O_{\text{aq}} \cdots O_{\text{aq}}$  distances are too close to each other to be resolved. However, by putting the  $O_{\text{aq}} \cdots O_{\text{aq}}$  distance to 2.890 Å and a temperature factor,  $b$ , of 0.0200 Å<sup>2</sup>, which are the normal values obtained for aqueous solutions containing high concentrations of solutes, an  $O_{\text{oxo}} \cdots O_{\text{aq}}$  distance of 2.873 Å was obtained which seems very reasonable. The S $\cdots O_{\text{aq}}$  distance refined 3.73(3) Å contained both distances to water oxygens hydrogen binding to oxo and peroxy oxygens, and they cannot be separated. It is assumed that the S- $O_{\text{oxo}} \cdots O_{\text{aq}}$  angle close to the tetrahedral angle, calculated to 3.62 Å from the obtained S- $O_{\text{oxo}}$  and  $O_{\text{oxo}} \cdots O_{\text{aq}}$  distances. The  $O_{\text{oxo}} \cdots O_{\text{aq}}$  distance indicates that the peroxodisulfate is a weak structure maker as the other oxosulfur anions studied, sulfate, sulfite and thiosulfate. The refined structure parameters from the LAXS measurement are summarized in Table 1, and the experimental and the calculated RDFs using the parameters given in Table 1 are shown in Figure S3 (see ESI†) together with the individual contributions from the hydrated thiosulfate and sodium ions and the aqueous bulk.

#### **Conclusions**

In the hydrated thiosulfate ion three water molecules are hydrogen bound to each of the oxygens and the terminal sulfur atom. The  $S_C-O$  and  $S_C-S_T$  bond distances, 1.479 and 2.020 Å, respectively, are slightly longer than in thiosulfate ions in the solid state due to the hydration. The hydrated thiosulfate ion shows asymmetry in the hydrogen bond strength with the hydrogen bonds to the oxygens stronger and the sulfur weaker than in pure water. The water exchange takes place directly at the oxygen and sulfur atoms in a similar way as previously found for the sulfate ion. The water molecules clustered around the terminal sulfur has a higher exchange rate than the oxygens showing that the terminal sulfur acts as a structure breaker while the oxygens are structures makers making the overall hydrogen bonding stronger around the thiosulfate ion than in pure water. The oxo sulfur anions dithionate or metabisulfate,  $S_2O_6^{2-}$ , disulfate or pyrosulfate,  $S_2O_7^{2-}$ , and peroxydisulfate,  $S_2O_8^{2-}$ , are most probably hydrated in similar way as the sulfate ion, while the dithionite,  $S_2O_4^{2-}$ , and disulfite,  $S_2O_5^{2-}$ , ions, with a lone electron-pair on both sulfur atoms or on one of them, respectively, are expected to be hydrated in a similar way the sulfite ion. It has been confirmed by a LAXS study that it hydrated in a similar way as the sulfate ion with S-O bond distances to the oxo and peroxy oxygens of 1.448(2) and 1.674(6) Å, respectively.

## Acknowledgments

We gratefully acknowledge the financial support from the Swedish Research Council and the Austrian Science Foundation.

**Supporting Information Available:** Additional information as noted in the text

## References

- (1) D. R. Rosseinsky, *Chem. Rev.* 1965, **65**, 467-490.
- (2) L. Eklund, T. S. Hofer, A. B. Pribil, B. M. Rode and I. Persson, *Dalton Trans.*, 2012, **41**, 5209-5216.
- (3) V. Vchirawongkwin, B. M. Rode and I. Persson, *J. Phys. Chem. B*, 2007, **111**, 4150–4155.
- (4) T. S. Hofer, H. T. Tran, C. F. Schwenk and B. M. Rode, *J. Comput. Chem.* 2004, **25**, 211-217.
- (5) M. Trinapakul, C. Kritayakornupong, A. Tongraar and V. Vchirawongkwin, *Dalton Trans.*, 2013, **42**, 10807-10817.
- (6) IUPAC Stability Constants Database (Sc-Database), Royal Society of Chemistry, Academic Software, 2000, and references therein.
- (7) [http://www.kodak.se/ek/uploadedFiles/Content/About\\_Kodak/Global\\_Sustainability/Health,\\_Safety\\_and\\_Environment/Publications\\_Library/J212ENG-0311.pdf](http://www.kodak.se/ek/uploadedFiles/Content/About_Kodak/Global_Sustainability/Health,_Safety_and_Environment/Publications_Library/J212ENG-0311.pdf).
- (8) R. K. Rath, N. Hiroyoshi, M. Tsunekawa and T. Hirajima, *Eur. J. Miner. Proc. Environ. Protection*, 2003, **3**, 344-352.
- (9) a/ F.-J. Leinweber and K. J. Monty, *J. Biol. Chem.*, 1963, **238**, 3775-3780; b/ M. Sooriyaarachchi, A. Narendran and J. Gailer, *Metallomics*, 2012, **4**, 960-967; c/R. M. S. Stocks, H. J. Gould, A. J. Bush, B. W. Dudley, Jr, M. Pousson, J. W. Thompson, *Otolaryngology Head Neck Surg.*, 2004, **131**, 115-119; d/ U. Kappler, C. G. Friedrich, H. G. Trüper, C. Dahl, *Arch. Microbiol.*, 2001, **175**, 102-111.
- (10) C. M. V. Stålhandske, I. Persson, M. Sandström and E. Kamienska-Piotrowicz, *Inorg. Chem.*, 1997, **36**, 3174–3182.
- (11) G. Johansson and M. Sandström, *Chem. Scr.*, 1973, **4**, 195-198.
- (12) M. Molund and I. Persson, *Chem. Scr.*, 1985, **25**, 197-197.
- (13) J. P. Chandler, *Behav. Sci.*, 1969, **14**, 81-82.
- (14) A. J. C. Wilson, Ed. *International Tables for Crystallography*; Kluwer Academic Publishers: Dordrecht, The Netherlands, 1995; Vol. C.
- (15) D. T. Cromer, *J. Chem. Phys.*, 1967, **47**, 1892-1893.
- (16) D. T. Cromer, *J. Chem. Phys.*, 1969, **50**, 4857-4859.
- (17) A. Warshel and M. Levitt, *J. Mol. Biol.*, 1976, **103**, 227-249.
- (18) M. J. Field, P. A. Bash, and M. Karplus, *J. Comp. Chem.*, 1990, **11**, 700-733.
- (19) J. Gao, *J. Am. Chem. Soc.*, 1993, **115**, 2930-2935.
- (20) D. Bakowies and W. Thiel, *J. Phys. Chem.*, 1996, **100**, 10580-10594.
- (21) M. Svensson, S. Humbel, R. D. J. Froese, T. Matsubara, S. Sieber, and K. Morokuma, *J. Phys. Chem.*, 1996, **100**, 19357-19363.
- (22) H. M. Senn and W. Thiel, *Curr. Opin. Chem. Biology*, 2007, **11**, 182-187.

- (23) H. Lin and D. G. Truhlar, *Theor. Chim. Acta*, 2007, **117**, 185-199.
- (24) B. M. Rode, T. S. Hofer, B. R. Randolph, C. F. Schwenk, D. Xenides and V. Vchirawongkwin, *Theor. Chim. Acta*, 2006, **115**, 77-85.
- (25) T. S. Hofer, A. B. Pribil, B. R. Randolph and B. M. Rode, *Adv. Quant. Chem.*, 2010, **59**, 213-246.
- (26) T. S. Hofer, B. M. Rode, A. B. Pribil and B. R. Randolph, *Adv. Inorg. Chem.*, 2010, **62**, 143-175.
- (27) Berendsen, H. J. C.; Postma, J. P. M.; van Gunsteren, W. F.; DiNola, A.; Haak, J. R. *J. Chem. Phys.* 1984, **81**, 3684-3690.
- (28) H. J. C. Berendsen, J. R. Grigera and T. P. Straatsma, *J. Phys. Chem.*, 1987, **91**, 6269-6271.
- (29) M. P. Allen and D. J. Tildesley, *Computer Simulation of Liquids*, Oxford Science Publications, Oxford, 1990.
- (30) T. H. Dunning, *J. Chem. Phys.*, 1970, **53**, 2823-2833.
- (31) E. Magnusson and H. F. Schaefer, *J. Chem. Phys.*, 1985, **83**, 5721-5726.
- (32) R. Ahlrichs, M. Bär, M. Häser, H. Horn and C. Kölmel, *Chem. Phys. Lett.*, 1989, **162**, 165-169.
- (33) F. H. Stillinger and A. Rahman, *J. Chem. Phys.*, 1978, **68**, 666-670.
- (34) P. Bopp, G.; Jansco and K. Heinzinger, *Chem. Phys. Lett.*, 1983, **98**, 129-133.
- (35) A. K. H. Weiss and T. S. Hofer, *RSC Adv.*, 2013, **3**, 1606-1635.
- (36) T. S. Hofer, H. T. Tran, C. F. Schwenk and B. M. Rode, *J. Comput. Chem.*, 2004, **25**, 211-217.
- (37) W. Humphrey, A. Dalke and K. Schulten, *J. Mol. Graph.*, 1996, **14**, 33-38.
- (38) J. Mähler and I. Persson, *Inorg. Chem.* 2012, **51**, 425-438.
- (39) A. B. Pribil, T. S. Hofer, B. R. Randolph and B. M. Rode, *J. Comput. Chem.* 2008, **29**, 2330-2334.
- (40) L. Eklund and I. Persson, *Dalton Trans.* 2014, **43**, 6315-6321.

**Table 1.** Mean bond distances,  $d/\text{\AA}$ , number of distances,  $N$ , temperature coefficients,  $b/\text{\AA}^2$ , and the root-mean-square variation (hw hh),  $l/\text{\AA}$ , in the LAXS studies of the aqueous sodium thiosulfate and peroxydisulfate solutions at room temperature, and from the QMCF MD simulation of the thiosulfate ion in aqueous solution.

Interaction	$N$	$d$	$b$	$l$	$d$	$l$
<i>Thiosulfate ion</i>						
LAXS					QMCF MD	
O <sub>thio</sub>	3	1.479(5)	0.0024(5)	0.069(7)	1.477	0.033
S <sub>C</sub> -S <sub>T</sub>	1	2.020(6)	0.0040(6)	0.089(7)	2.017	0.046
O <sub>thio</sub> ⋯O <sub>aq1</sub>	9	2.854(10)	0.022(2)	0.210(2)	2.852	0.076
S <sub>T</sub> ⋯O <sub>aq2</sub>	3	3.24(5)	0.063(9)	0.35(3)	3.552	0.289
S <sub>C</sub> ⋯O <sub>aq1</sub>	9	3.622(7)	0.034(2)	0.26(1)	3.786	0.170
S <sub>C</sub> ⋯O <sub>aq2</sub>	3	4.36(6)	0.049(7)	0.31(2)	4.084	0.123
Na-O <sub>aq</sub>	6	2.42(2)	0.0254(8)	0.23(1)		
O <sub>aq</sub> ⋯O <sub>aq</sub>	2	2.890(2)	0.0200(3)	0.20(2)		
<i>Peroxydisulfate ion</i>						
S-O <sub>oxo</sub>	6	1.448(3)	0.0027(3)	0.073(4)		
S-O <sub>peroxo</sub>	2	1.674(6)	0.0060(8)	0.110(7)		
O <sub>thio</sub> ⋯O <sub>aq</sub>	3	2.873(5)	0.0169(7)	0.184(4)		
S⋯O <sub>mean</sub>	11	3.73(1)	0.020(1)	0.20(1)		
Na-O <sub>aq</sub>	6	2.432(9)	0.0245(9)	0.221(4)		
O <sub>aq</sub> ⋯O <sub>aq</sub>	2	2.890(2)	0.0200(3)	0.200(2)		

**Table 2.** Atomically centered Mean residence times, MRTs, in ps and average number of exchanges required to achieve one lasting exchange longer than 0.5ps,  $R_{ex}$ , of water molecules in the hydrated thiosulfate from simulations on HF theory level

Atom	$t^*=0.0ps$		$t^*=0.5ps$			Note
	MRT	$N_{ex}/10ps$	MRT	$N_{ex}/10ps$	$R_{ex}$	
O <sub>thio</sub>	0.45	171	3.06	19.0	9.0	a
O <sub>thio</sub>	0.50	153	3.85	15.2	10.1	a
O <sub>thio</sub>	0.46	167	4.01	14.4	11.6	a
S <sub>t</sub>	0.4	306	2.43	45.6	6.7	b

<sup>a</sup> More stable than pure water.

<sup>b</sup> More stable than water, but less stable than oxygens.

**Table 3.** Mean residence times, MRTs,  $\tau_{0.5}$  in ps and the sustainability coefficients,  $S_{ex}$ , of water molecules in the hydrated thiosulfate, sulfite, sulfate and phosphate ion and bulk water from simulations on HF theory level.

Hydrated ion	$\tau_{0.5}$	$N_{ex}^{0.5}$	$N_{ex}^{0.0}$	$1/S_{ex}$	Reference
Sulfite	3.2	59	346	5.9	2
Sulfate	2.6	54	399	7.4	3
Phosphate	3.9	42	132	3.1	39
Bulk water	1.7	24	269	11.2	4

**Table 4.** Long( $\tau_L$ ) and short( $\tau_S$ ) parameters of the hydrogen bond correlation functions, the intermittent  $C_{HB}(t)$  and the continuous  $S_{HB}(t)$ , the long parameter of the  $S_{HB}(t)$  is equal to the average lifetime of the hydrogen bond. The parameters show that the average bond duration with oxygen as a acceptor is about twice that of a bond with sulfur as acceptor.

Hydrogenbond acceptor	$C_{HB}(t)$		$S_{HB}(t)$	
	$\tau_L$	$\tau_S$	$\tau_L$	$\tau_S$
Sulfur	1.161	0.0146	0.223	0.0281
Oxygen <sub>A</sub>	2.054	0.1048	0.317	0.0124
Oxygen <sub>B</sub>	1.989	0.0590	0.400	0.0488
Oxygen <sub>C</sub>	2.694	0.1527	0.447	0.0780
Oxygen average	2.246	0.1055	0.388	0.0464

## Legends to Figures

**Figure 1.** LAXS, thiosulfate ion. Top: the individual peak shapes for all contributing species in the 1.5066 mol·dm<sup>-3</sup> aqueous solution of sodium thiosulfate, the hydrated thiosulfate ion (orange line), hydrated sodium ion (brown line) and the aqueous bulk (green line). (b) Experimental  $D(r) - 4\pi r^2 \rho_0$  (red line); model (black line), the modelled distances are given in Table 2; difference (blue line). Bottom: reduced LAXS intensity function,  $si(s)$  (thin black line); model  $si_{\text{calc}}(s)$  (red line).

**Figure 2:** Angular Radial Distribution function, showing the sulfite (top), thiosulfate (middle) and sulfate (bottom) ions. The occupancy of thiosulfate ion is seen as asymmetric, but to a lesser extent as the sulfite.

**Figure 3:** Angle vs distance plot and hydrogen bond correlation function  $C_{\text{HB}}(\tau)$ ,  $\text{O}_{\text{thiosulfate}}$  to water hydrogen bonds (black),  $\text{S}_{\text{T}}$  to water hydrogen bonding (Red), the equation  $C_{\text{HB}}(\tau) = a_0 e^{-\tau/\tau_1} + (1-a_0) e^{-\tau/\tau_2}$  was fitted to respective sampling (dashed lines). Clearly noticeable is the different in hydrogen bond mean lifetimes with  $\text{S}_{\text{T}}$  again behaving as weak structure breaker and  $\text{O}_{\text{thio}}$  as structure makers.

**Figure 4:** Volume map of the first hydration shell water and thiosulfate ion. Coloured by charge.

**Figure 5:** Oxygen densities surrounding the central ion in planes cutting perpendicular to the  $C_{3v}$  axis of the central ion and spaced 1 Å apart. With the solute overlaid in RGB over the solvent CMYK color scheme and letting the central image be a plane that cuts through the center of  $\text{S}_{\text{A}}$  and then moving along the axis up (left and towards the top) or down (right and towards the bottom)

**Figure 6:** Coordination number distribution of thiosulfate, obtained by registering each water oxygen atoms located within the first shell of either  $\text{O}_{\text{thio}}$  or  $\text{S}_{\text{T}}$ . The resulting average coordination number amounts to 12.5.

Figure 1

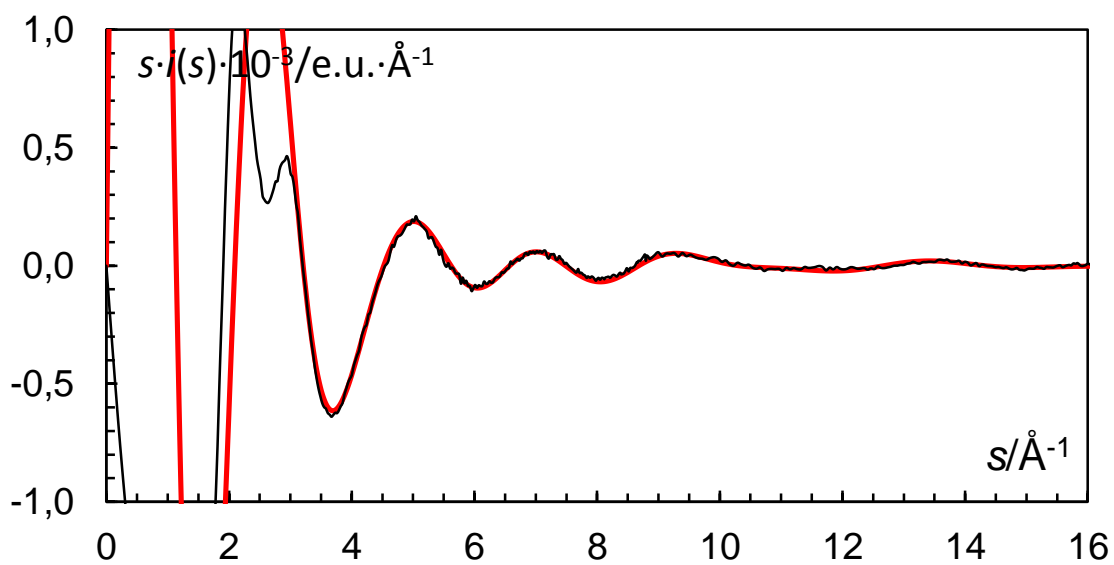
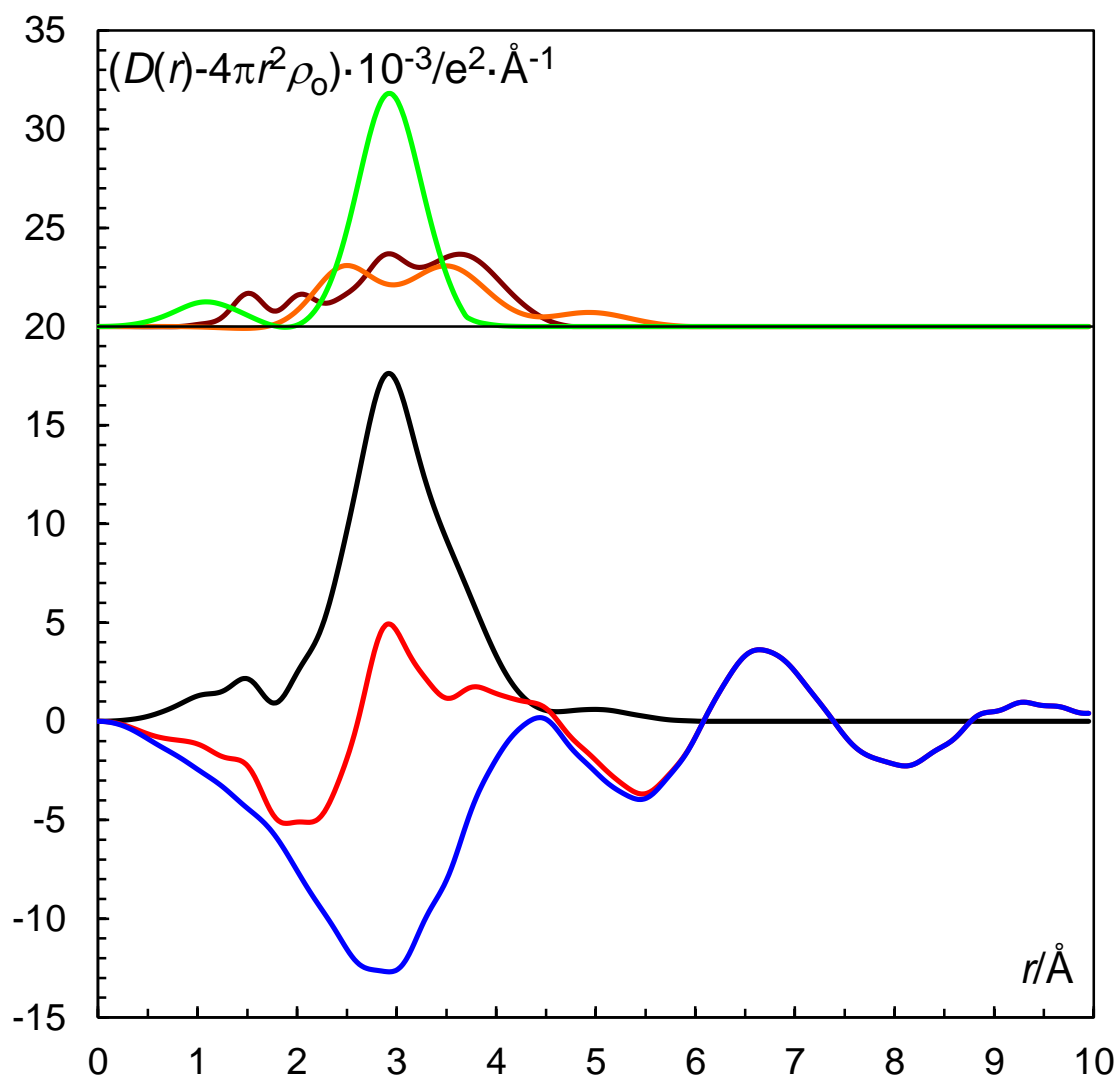


Figure 2

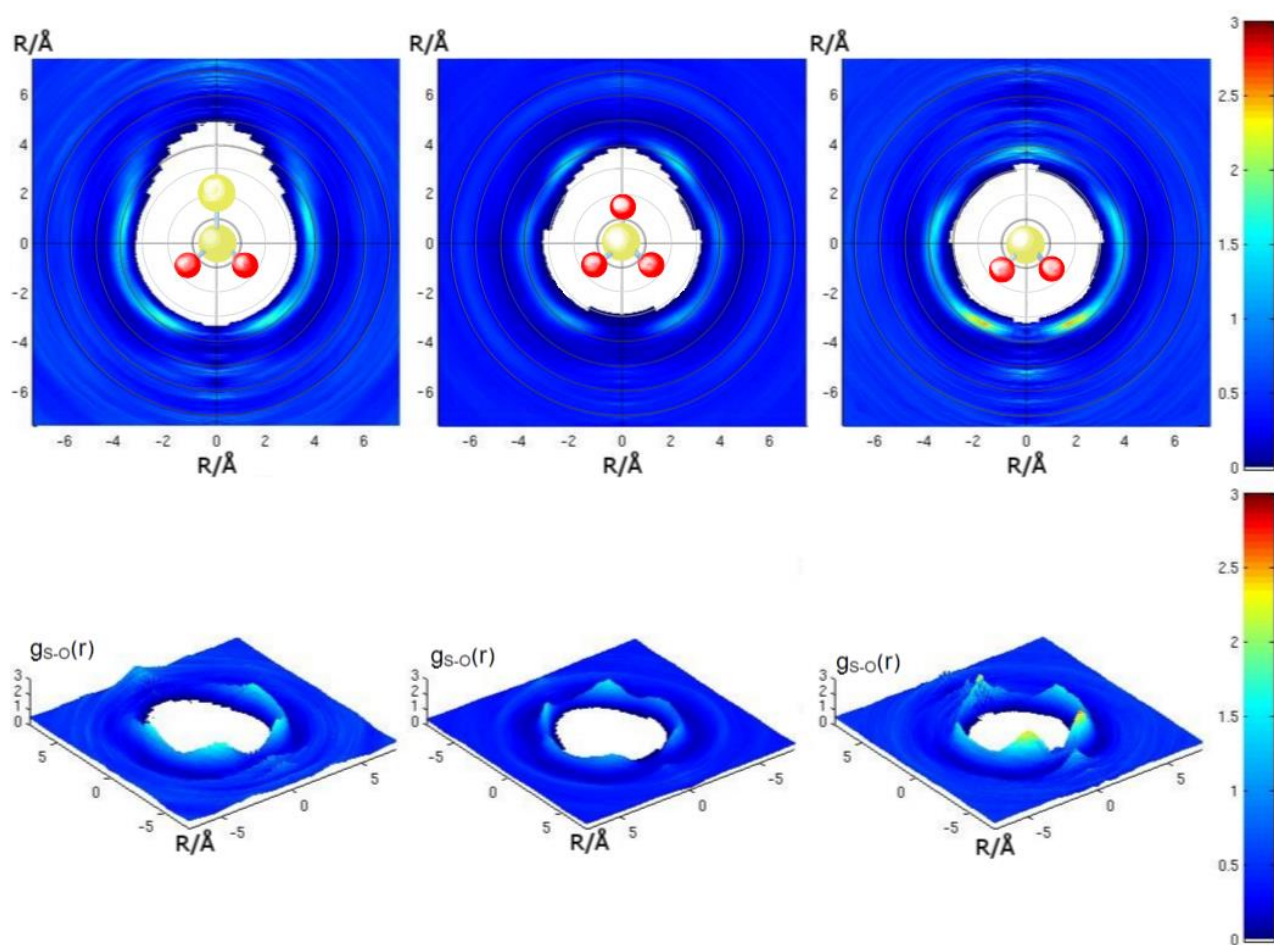
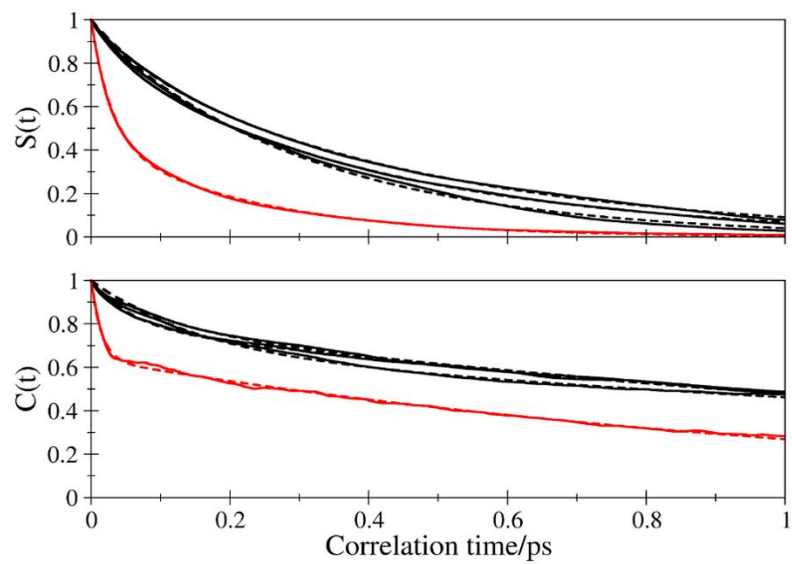
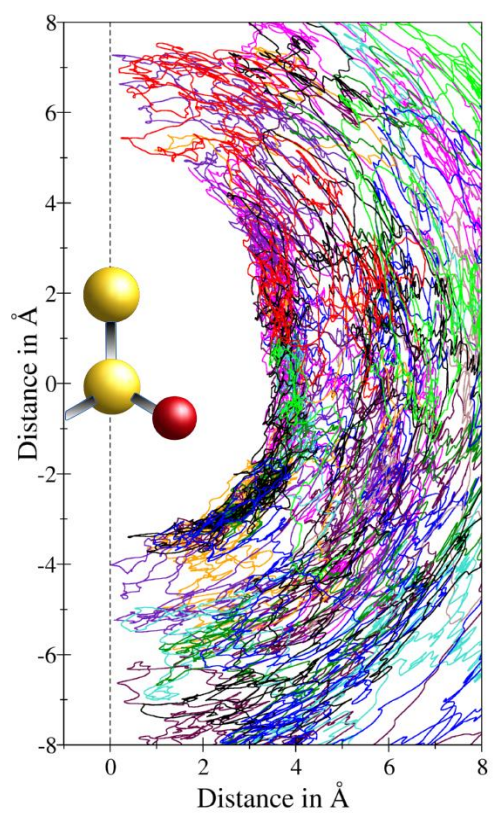


Figure 3



**Figure 4**

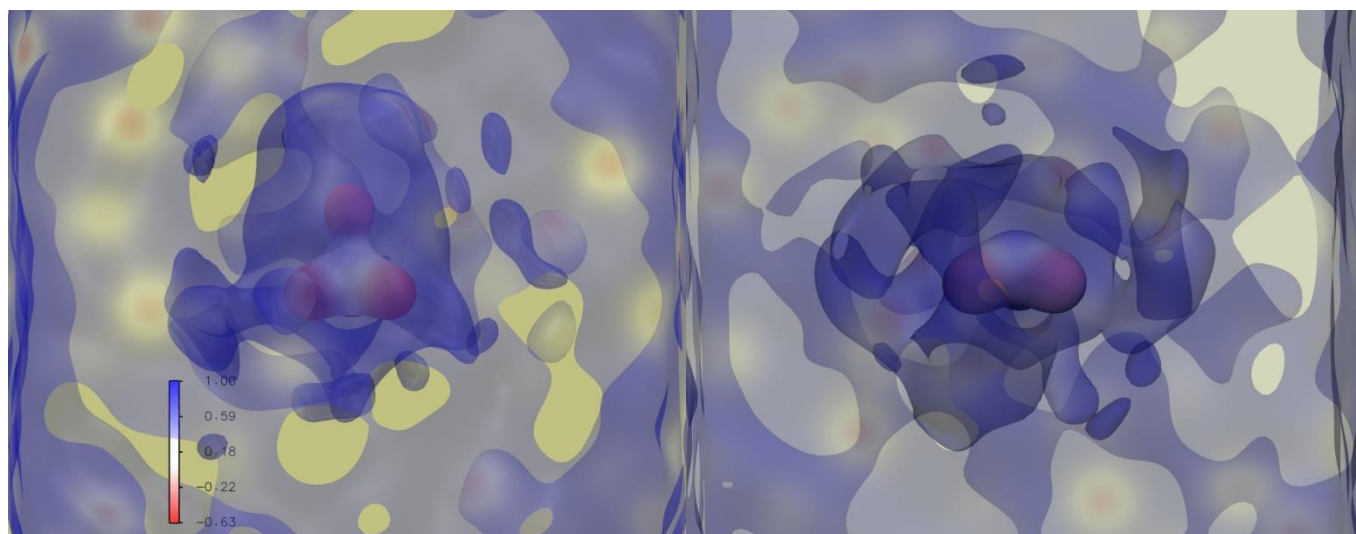
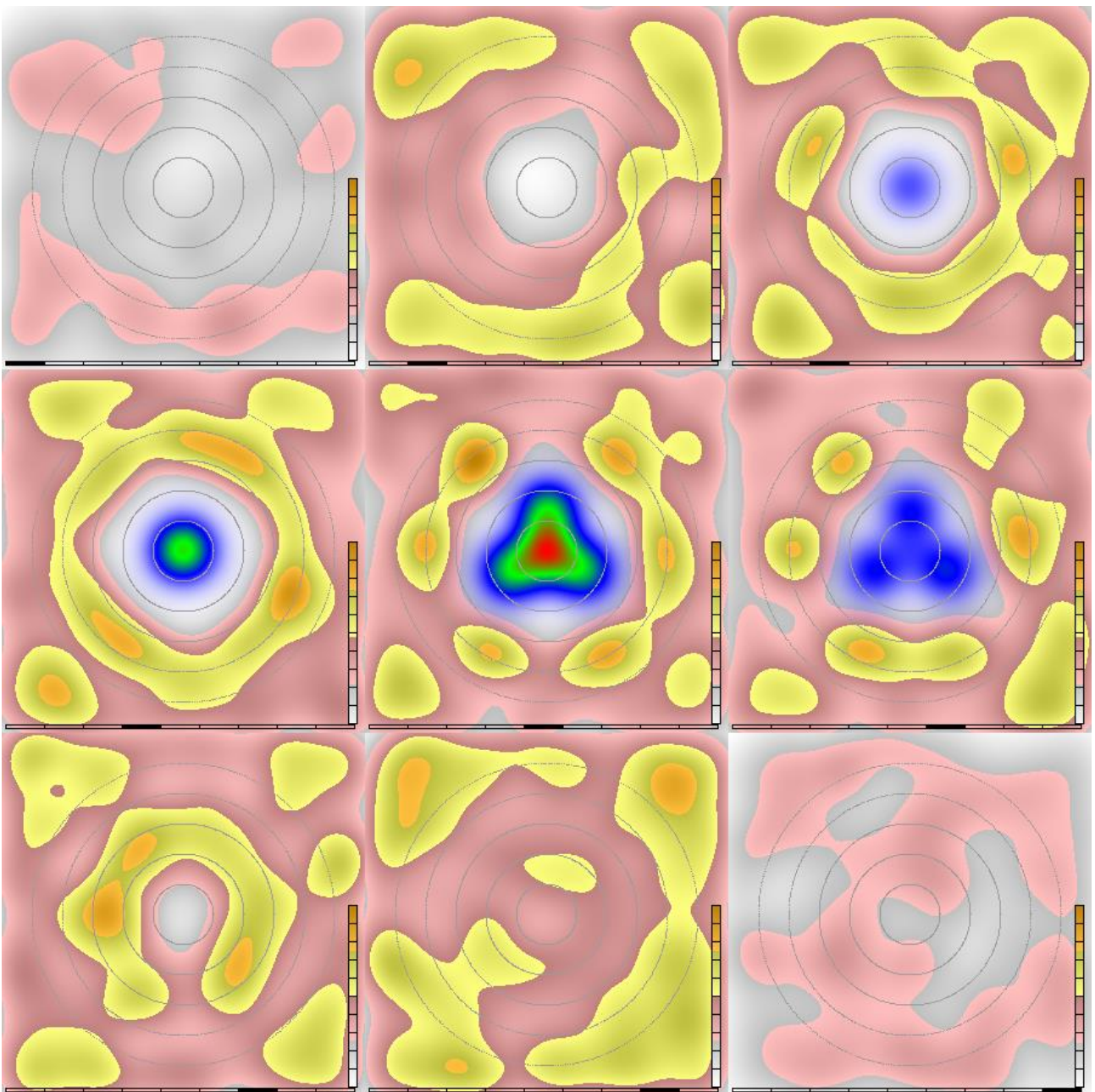
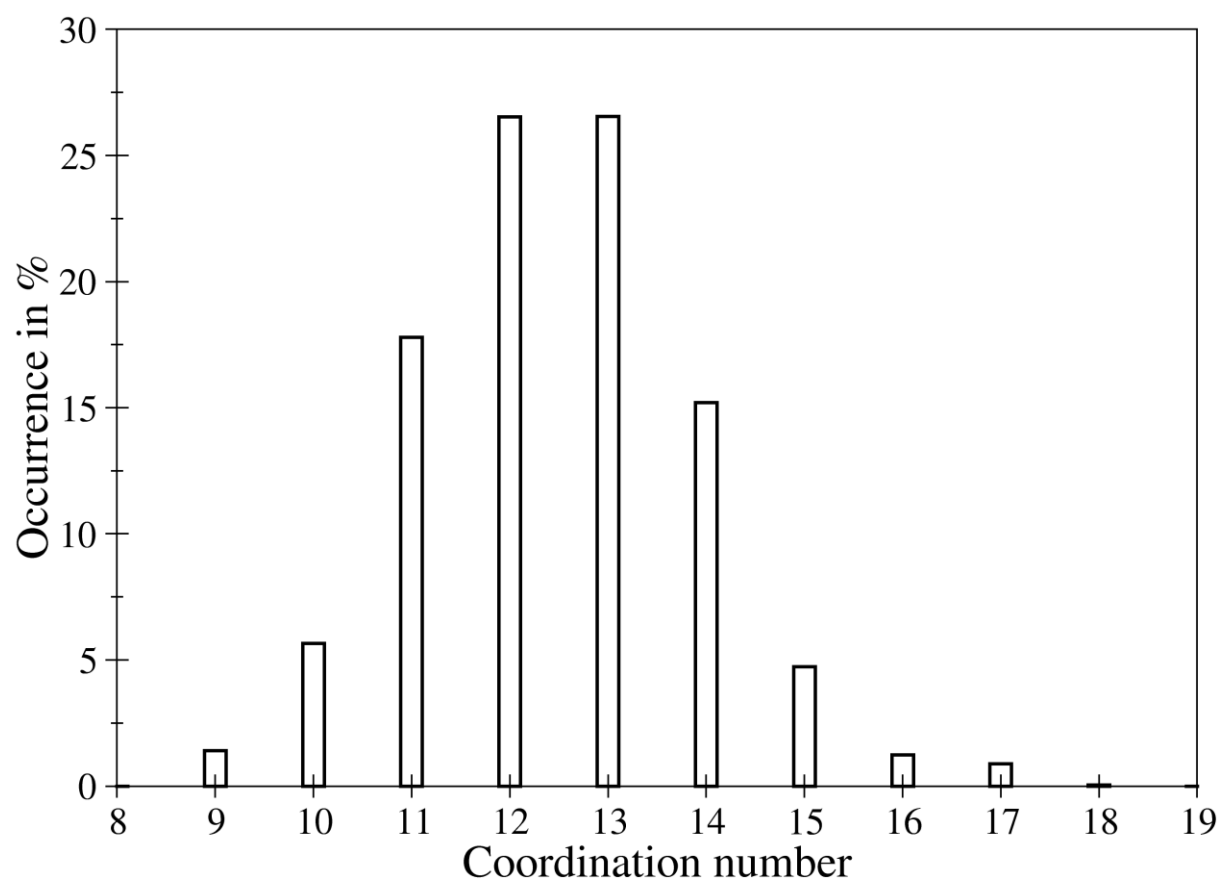


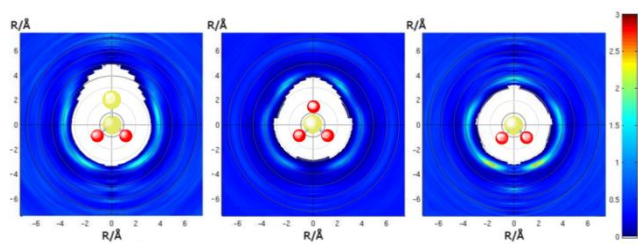
Figure 5



**Figure 6**



## Graphical Abstract



## Synopsis

Experimental and simulation data of the thiosulfate ion show large similarities in hydration structure and mechanism with the sulfate ion but with weaker hydration of the terminal sulfur atom in thiosulfate.